Decarbonizing heat with PV-coupled heat pumps supported by electricity and heat storage: Impacts and trade-offs for prosumers and the grid

Pena Bello, Alejandro; Schuetz, Philipp; Berger, Matthias; Worlitschek, Jörg; Patel, Martin; Parra Mendoza, David

How to cite

PENA BELLO, Alejandro et al. Decarbonizing heat with PV-coupled heat pumps supported by electricity and heat storage: Impacts and trade-offs for prosumers and the grid. In: Energy Conversion and Management, 2021, vol. 240, n° 114220. doi: 10.1016/j.enconman.2021.114220

This publication URL: https://archive-ouverte.unige.ch/unige:153868
Publication DOI: 10.1016/j.enconman.2021.114220

Energy Conversion and Management 240 (2021) 114220

Contents lists available at ScienceDirect

Energy Conversion and Management

journal homepage: www.elsevier.com/locate/enconman

Decarbonizing heat with PV-coupled heat pumps supported by electricity and heat storage: Impacts and trade-offs for prosumers and the grid

Alejandro Pena-Bello [a,*], Philipp Schuetz [b], Matthias Berger [b], Jörg Worlitschek [b], Martin K. Patel [a], David Parra [a]

[a] Energy Efficiency Group, Institute for Environmental Sciences and Forel Institute, University of Geneva, Boulevard Carl-Vogt 66, 1205 Genève, Switzerland
[b] Lucerne University of Applied Sciences and Arts, School of Engineering and Architecture, Technikumstrasse 21, 6048 Horw, Switzerland

ARTICLE INFO

Keywords:
PV
Heat pump
Battery
Heat storage
Capacity-based tariff

ABSTRACT

Heat pumps play an important role in decarbonizing the heating supply of buildings and they allow to increase the self-consumption of PV electricity, especially when supported by electricity or heat storage. In this study, we develop an open-source model to optimize PV-coupled heat pumps, with and without electricity and heat storage, and we compare their performance for three types of single-family houses with different thermal envelope quality paired with 549 electricity profiles. We analyze trade-offs between prosumer benefits and grid impacts, namely bill minimization, and maximum grid relief, depending on the type of storage and incentives for grid peak reduction (i.e., a capacity-based tariff). We conclude that the use of heat storage reduces the levelized cost of meeting the electricity demand between 13–26% compared to the baseline case without storage, in particular when heat pumps are used for both space heating and domestic hot water (DHW). Regarding total self-consumption rates, both storage technologies, namely batteries and hot water tanks (which supply both space heating and DHW) achieve similar rates ranging between 30–39%. In contrast, batteries are found to be very effective in reducing the peak demand (14–17% compared to the baseline scenario), but only if the retail tariff has a capacity-based component. Interestingly, the quality of the envelope plays a key role and heat pumps can double the power peak demand in poorly insulated houses, with thermal storage increasing the power peak demand further up to 8%, compared to the baseline, regardless of the storage technology. Thus, we conclude that policy makers should promote thermal retrofitting of the building stock to avoid the upgrading of the distribution grid.

1. Introduction

Heat supply is dominated by fossil fuels and in 2019, only 11% of the heat was supplied by renewable energy sources worldwide [1]. This fossil dependency was equivalent to a contribution of 40% to global CO2 emissions (equal to 13.3 gigatonnes) in the same year. In Switzerland, space heating demand needs to be significantly reduced as it represents more than two thirds of the total final energy demand in the built environment [2]. Energy retrofitting programs together with heat pumps are crucial elements of the Swiss Energy Strategy 2050. Heat pumps operate with much higher efficiency, referred to as coefficient of performance (COP), than condensing boilers or furnaces, allowing to reduce the energy consumption in buildings by 15–70% [3].The Swiss Federal Office of Energy anticipates that the number of heat pumps sold per year will double by 2030, reaching 40.000 units p.a. [4]. However, most heat pumps are installed in new buildings while the retrofitting rate in existing buildings is very low (less than 1% p.a. [5]) representing the main challenge for heat pump diffusion.

Solar photovoltaics (PV), which so far has mainly be used to decarbonize electricity supply, can be key to also decarbonize the heating sector [1,6]. PV modularity and cost-reduction empower consumers that can now generate their own electricity, becoming prosumers, thereby

Abbreviations: **PV**, Photovoltaics; **HP**, Heat pump; **FiT**, Feed-in Tariff; **COP**, Coefficient of performance; **ToU**, Time of use; **SFH**, Single-family house; **DHW**, Domestic hot water; **SH**, space heating; **NPV**, Net present value; **CF**, Cash flow; **LCOE**, Levelized cost of meeting the electricity consumption; **CAPEX**, Capital expenditure; **OPEX**, Operating expenditure; **SC**, Self-consumption; **SS**, Self-sufficiency; **PVSC**, PV self-consumption; **DLS**, Demand load-shifting; **DPS**, Demand peak shaving; **SOC**, State of charge; **DoD**, Depth of discharge; **ILR**, Inverter load ratio; **NMC**, Lithium nickel manganese cobalt oxide.

* Corresponding author.
E-mail address: alejandro.penabello@unige.ch (A. Pena-Bello).

https://doi.org/10.1016/j.enconman.2021.114220
Received 12 January 2021; Accepted 24 April 2021
Available online 24 May 2021

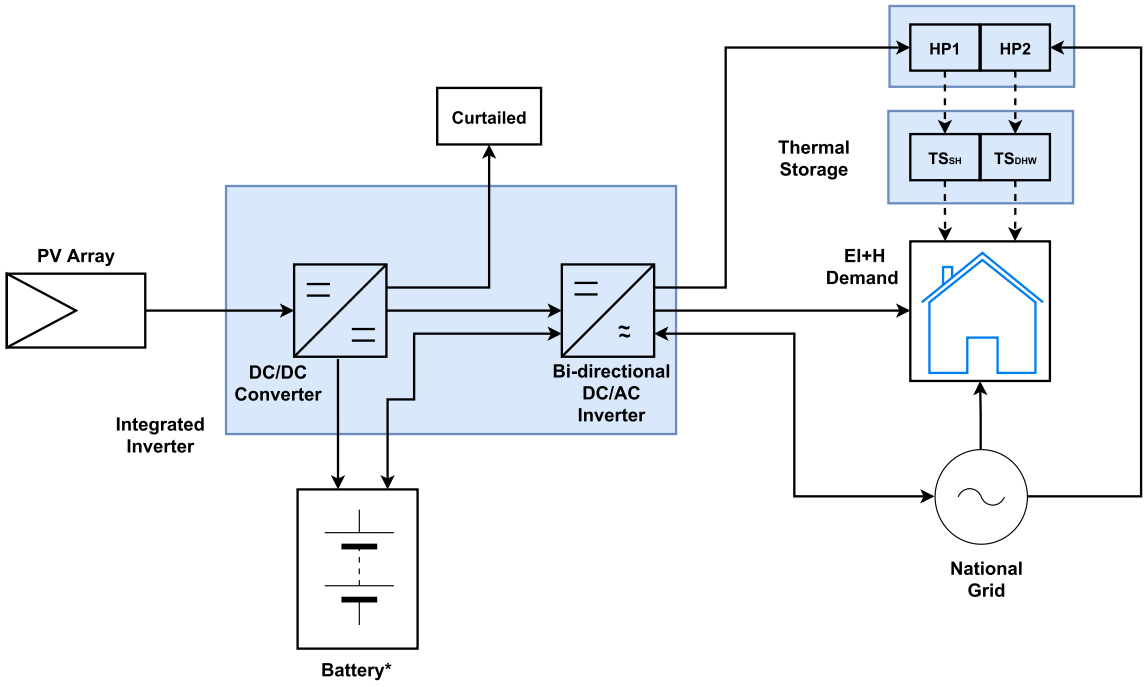

Fig. 1. Schematic representation of a PV-coupled heat pumps supported by electricity and/or heat storage used in this study. The arrows indicate the direction of possible electricity and heat flows between the individual components. The supply of domestic hot water (DHW) and space heat (SH) is modelled with two different heat pumps (HP) whereas, in reality a single heat pump is used. TS stands for thermal storage.

directly contributing towards the energy transition. However, the expansion of decentralized rooftop PV systems poses a challenge to the power sector. Unlike conventional centralized generation, PV production cannot be supplied on-demand without incurring additional costs and devices. Moreover, for high distributed PV penetration levels, grid operators may be forced to use rapid and expensive ramp-up of centralized power to match the demand (this is referred to as the duck-curve problem [7]), to shut-down baseload plants and/or to curtail PV electricity to avoid voltage issues at the low and medium voltage grid levels [8–10].

In order to supply PV electricity on-demand and minimize grid impacts, there are a number of flexibility strategies that allow to increase PV self-consumption [11,12]. In this article, we focus on heat pumps supported with electricity (batteries) and heat (hot water tanks) storage. Heat pumps can increase PV self-consumption and simultaneously decarbonize space heating and domestic hot water (DHW) supply, which so far mainly relies on fossil fuels [13]. When using local PV generation, heat pumps can perform with high COP values (e.g., above 3) due to relatively high ambient temperature at midday. Regarding storage, in addition to shift PV generation, storage can also be used to exploit time-varying electricity prices, i.e. charging at low prices and discharging at high prices (prices in USD/kWh_{el}), referred to as demand load shifting (DLS) [14,15]. Furthermore, storage can be used to perform demand peak shaving (DPS), which consists of discharging for a short period of time, e.g., 15-min, to reduce the maximum power exchanged with the grid (in kW terms). DPS requires that the retail tariffs include a capacity-based component (USD/kW_{el}) in addition to the volumetric component (USD/kWh_{el}) [16,17].

Considering the high interest in both PV self-consumption and heat decarbonization, we focus on PV-coupled heat pumps assisted with electricity and heat storage to meet both electricity and heat demand in single-family houses. This is an important topic because the diffusion of PV and heat pumps is crucial for the energy transition but influences the nationwide electricity peak demand, distribution grid stability, and electricity infrastructure upgrade cost [18]. Thus, in this study we combine three storage applications for electric and heat storage, namely, PV self-consumption, DLS and DPS.

2. Literature review

Low carbon technologies such as PV, heat pumps, batteries and hot water tanks have been a focal topic of the previous literature, however, control strategies of all the above-mentioned technologies combined in smart houses has been rather limited. When analyzing control strategies for heat pump integration, a smart response to prices was considered [19–21]. Studies focusing on PV-coupled heat pumps give priority to the increase of PV self-consumption [22–24], and combinations of applications have been hardly considered, except for PV self-consumption and demand peak shaving [25]. However, these studies did not consider the added flexibility of electricity or heat storage.

Very few studies addressing heat pumps have so far analyzed the combinations of applications using energy storage. Liu et al. assessed the impact of heat pumps on the battery schedule performing under time-of-use (ToU) tariffs [26]. They recommended to conduct a whole-system analysis to maximize PV self-consumption while reducing battery capacity, which is achieved by directly using more PV electricity in the heat pump. Terlouw et al. also considered ToU tariffs when comparing electricity and heat storage to minimize the electricity bill and CO_2 emissions at the individual household and community levels [27]. Large hot water tanks shared by the community and small individual batteries help to minimize the bill for communities and individual houses, respectively. Another study by Pimm et al. found that small batteries can mitigate the grid impacts of heat pumps, ensuring that peak flow values do not increase after the heat pump installation [28]. However, the authors did not consider any economic aspects nor economic incentives for peak demand reduction.

Since the space heating demand of a residential building largely depends on its insulation, some authors have compared different reference buildings [29] and assessed underfloor heating and radiators [30]. However, PV-coupled heat pumps assisted with electricity and heat storage and their trade-offs for prosumers and distribution grids, in terms of PV self-consumption and demand peak shaving, have not yet

been studied as a function of the envelope quality. To our knowledge, this is the first paper proposing a method to evaluate PV-coupled heat pumps, and to compare their performance when assisted with electricity and heat storage, both individually and combined, for houses with different envelope quality. The proposed open-source model optimizes the heat pump and energy storage operation for a whole year and the results are then scaled over a time period of 30 yr (corresponding to the PV lifetime). Importantly, we analyze the trade-offs between prosumer benefits and impacts on the grid, using three types of houses with different thermal insulation, which are coupled with 549 electricity profiles to provide robust results backed by statistical tests. Our open-source model is applied to houses in Geneva, Switzerland, however, it can be adjusted to locations with temperate climate and fast diffusion of PV and heat pumps.

The remainder of this paper is structured as follows. The input data and methods are presented in Section 3 which describes he system configuration, as well as the optimization setup and the techno-economic indicators. Section 4 presents the optimization results as a function of the system configuration, building type and electricity tariff. Section 5 is a discussion of the implications of our results and finally, Section 6 presents the main conclusions.

3. Input data and method

First, we define the input data for the model in Section 3.1, including various types of houses, electricity and heat demand data, as well as the PV generation and the electricity tariff structure. Secondly, the optimization is described in detail in Section 3.2, as well as the PV-coupled heat pump configurations including storage. Finally, we present the techno-economic performance indicators in Section 3.4. Fig. 1 is a schematic representation of a PV-coupled heat pump as considered in this study. We use data from 2017 across this study.

3.1. Input data

3.1.1. Thermal characteristics of the houses

Based on the reference framework for buildings and space heating simulations of the International Energy Agency [31], we compare PV-coupled heat pumps in three archetypical single-family houses (SFH) with identical living area (a two story SFH with 140 m^2 of heated floor area) but different heat demand, corresponding to 15, 45 and 100 kWh_{th}/m^2 p.a., referred to as SFH15, SFH45 and SFH100 respectively. These values represent a very well insulated recent building (i.e., Minergie-P in Switzerland or Passivhaus in Germany), a modern building from 2000–2010 (i.e., with a good thermal insulation of the building envelop) and a renovated old building (before 1980) or equivalently, a building from around 1980–1990 (i.e., poorly insulated) respectively [2]. The SFH15 and SFH45 are assumed to have underfloor heating running at up to 35 °C, which serves as heat storage directly coupled to the heating system. As for the SFH100, modern low-temperature radiators operated at around 50 °C are assumed [31–33], i.e., without storage capacity. Space heat demand and DHW demand are presented in Section 1 of the SI.

3.1.2. Electricity, heat demand and PV generation

In order to model the mismatch between PV generation and total electricity demand (including the consumption from appliances and the heat pump), we use data of 549 houses with 15-min temporal resolution monitored in single-family houses in Western Switzerland [34]. Since only electricity consumption was monitored, we link each electricity profile to SFH15, SFH45 and SFH100 heat demands, in order to analyze all possible combinations of electricity and heat consumption, thereby considering that electricity and heat demand are not directly correlated (if the heating system is not electric).

The space heating and DHW demands for the three types of houses are calculated using a calibrated dynamic simulation tool [35]. The simulation tool calculates the dynamics of the building and energy system by solving the coupled differential equations of the individual components using a Runge–Kutta integrator. The DHW draft profile is calculated using the DHWcalc tool [36] simulating the draft profile of a family with two adults and two children. The simulation framework is implemented in C++ with Visual Studio Community 2017 from Microsoft and the coupled differential equations models are solved in a program implemented using the same programming language. Further information can be found in Section 1 of the Supplementary Information (SI) and in Ref. [35].

We simulate PV generation using a standard one-diode model [37,38] and PV technology with a nominal efficiency of 18.6% [39], representative of the current technology state. A sky model is used to transform satellite data of horizontal solar irradiance into irradiance with a tilt angle of 30° and facing south, which corresponds to the PV system orientation [40]. Outdoor temperature was collected locally in Geneva by the University of Geneva [41]. The model also includes a maximum power point tracker system, as is the case of most PV systems to maximize the output regardless of the environmental conditions (temperature and solar irradiance). Finally, we consider PV systems with a nominal capacity equal to the median size of the empirical PV distribution across Switzerland, corresponding to 4.8 kWp [42]. The capacity factor of the modelled PV system is 16.1%, which is in line with other results for the same location (e.g., 15.7% in renewables.ninja for 2019) [43]. The specific technology costs for PV, battery, heat pumps and hot water tanks are given in Table A.1.

Table 1
Electricity tariff components depending on the bill structure used in this study. The peak time occurs from 7 a.m. to 10 p.m. on weekdays and from 5 p.m. to 10 p.m. on weekends. The export value corresponds to the wholesale price in the EPEXSPOT market. The price shown corresponds to the average wholesale price.

Name		Units	Geneva	Based on
ToU tariff	On-peak	USD/kWh_{el}	0.259	Energy
	Off-peak	USD/kWh_{el}	0.165	Energy
Export price		USD/kWh_{el}	0.047	Energy
Capacity-based tariff		*USD*/kW_{el}/*month*	9.39	Power

3.1.3. Electricity tariffs

Electricity prices used in this study are based on available tariffs offered by the local utility company in Geneva. We consider a ToU tariff, normally offered for heat pumps. The export PV price is assumed to be equal to the wholesale electricity price (based on the prices from the day-ahead European Power Exchange) as is the case for traditional electricity generators.

Importantly, we also test the impact of adding a capacity-based tariff (also referred to as demand charges) to today's tariff which is typically only volumetric. A capacity-based tariff (in USD/kW_{el}) represents a charge that is proportional to the maximum peak power, considering import from and export to the grid. To reduce the grid impacts of PV, heat pumps and electric vehicles and enabled by the deployment of smart meters, capacity-based tariffs are already being tested in some countries, e.g., France, Belgium, Austria and Sweden [44,45]. In this study, a capacity-based tariff is modelled as 9.39 *USD*/kW_{el}/*month*, while ensuring that the original overall electricity bill remains unchanged. This is achieved after reducing the volumetric component of the double tariff by 20%. Table 1 provides all the relevant tariff data depending on the bill structure.

3.2. Optimization modeling

We propose a daily schedule optimization (starting at midnight) of the PV-coupled heat pumps (see Fig. 1). Every optimization was run for one year and then the results are scaled over a time period of 30 years,

Table 2
Heating system characteristics depending on the building type with identical heated floor area of 140 m^2 for a two stories single-family house.

Heat Pump	SFH15	SFH45	SFH100
Required heat at the design point [kW_{th}]	2.4	4.9	10.6
Supply temperature at the design point [°C]	35	35	50
Temperature difference at the design point [K][a]	46	46	61
Generated heat demand at the design point [kW_{th}]	4	4.8	9.7
HP Thermal capacity [kW_{th}]	4	6	16
Working fluid	410a	410a	410a
Maximum electric demand at the design point [kW_{el}]	1.7	2	6.6
Backup heater [kW_{th}][b]	2	4	4
Space heating storage system	**SFH15**	**SFH45**	**SFH100**
Type of storage	Existing[c]	Existing[c]	New[d]
Specific capacity of the heat release of storage [kJ/K]	40000	40000	6300
Maximum ΔT [K]	1.5	1.5	10
Active building storage capacity based on possible temperature difference [kJ]	60000	60000	63000
Equivalent water capacity @ 10 K ΔT [l]	≈ 1500	≈ 1500	1500
DHW storage system	**SFH15**	**SFH45**	**SFH100**
Maximum ΔT [K]	20	20	20
Storage capacity based on temperature difference [kJ]	16800	16800	16800
Water capacity [l]	200	200	200

[a] The design point was used to size the heat pump, using IEA methodology [13].
[b] An electric backup heater with a COP of 1 is used to meet the peak heat demand, especially when there is simultaneous DHW and space heating demands.
[c] An existing space heating storage refers to an active heat building storage, which is directly coupled to the heating system, i.e., the thermal capacity of the heating system (radiator or underfloor heating), contrary to the passive building storage which refers to the heat storage capacity of the activatable building mass (which is not considered in this study) [49].
[d] A new storage refers to a technical storage, which is the name given to a heat storage unit that is installed in the building as an additional device [49].

corresponding to the lifetime of the PV system [46]. We consider replacements for all the components of the system (see SI Section 5 for more information). The open-source Linear Programming model developed by Pena-Bello et al. [34] is extended in this study to couple heating with heat pumps in combination with heat storage and electricity storage. We model eight PV-coupled heat pumps with and without thermal and electricity storage (see subsection 3.2.4) using the open-source programming language Python. To formulate the optimization problem, we use the Pyomo package [47], a Python-based optimization modeling language and to solve the scheduling optimization problem we use CPLEX, an optimization software package developed by IBM. The model can be found in githubhttps://github.com/alefunxo/BASOPRA_HP. Perfect forecast is assumed for electricity and heat demand, PV generation and wholesale prices in order to determine the maximum economic potential regardless of the chosen forecast strategy. The objective function is the minimization of the electricity bill which also includes a power-based component if a capacity-based is included, as is indicated in Eq. (1).

$$C = min\left(\overbrace{\sum_{i=0}^{t}\left(E_{grid_i}\cdot\pi_{import_i} - E_{PV-grid_i}\cdot\pi_{export_i}\right)}^{\text{Energy-based tariff}} + \underbrace{\left(P_{max-day}\cdot\pi_{capacity}\cdot PS\right)}_{\text{Power-based tariff}}\right) \quad (1)$$

Here, the energy-based tariff is given by E_{grid_i} [kWh_{el}] which is the electricity drawn from the grid; π_{import_i} is the import price (i.e., retail price, in USD/kWh_{el}); $E_{PV-grid_i}$ [kWh_{el}] is the PV-electricity exported to the grid; and π_{export_i} is the export price (in USD/kWh_{el}, assumed to be the wholesale price in this study). All these variables have the sub-index i representing every time step (corresponding to 15-min) from 0 up to 96 per day (represented by t). The capacity-based tariff is given by $P_{max-day}$ [kW], which is the maximum power required from the grid throughout the day; $\pi_{capacity}$ is the capacity-based tariff (in USD/kW_{el}/day); and PS is a boolean variable which indicates the presence of the capacity-based tariff (to enable demand peak shaving). The objective function is subject to various technical and energy system-related constraints which are presented hereafter. The model validation can be found in Section 6 of the SI.

3.2.1. Heat pump modeling

We model a bivalent heat pump, comprising an air to water heat pump and an electric backup heater connected in series to meet all heating requirements when the heat pump cannot meet them due, for instance, to under-sizing or to extremely low temperatures. The characteristics of the heating system as a function of the type of house are presented in Table 2. The sizing of the heat pump as well as the specification of the supply and return temperatures follow the methodology presented by the IEA [31] and are presented in the Section 2 of the SI. A detailed list of model parameters and variables is presented in Table A.2.

From a modeling perspective, the heat pump is virtually split into two parts which separately provide space heat and DHW. By analogy with real heat pumps, the two virtual parts cannot work at the same time and operate at different outlet temperatures. Eqs. (2)–(5) describe the heat pump constraints. The constraint of electricity demand is shown in Eq. (2), where E_{hp_i} is the electricity required by the heat pump, while E_{PV-hp_i} [kWh_{el}], $E_{batt-hp_i}$ [kWh_{el}] and $E_{grid-hp_i}$ [kWh_{el}] are the PV electricity supplied to the heat pump, the battery and the grid, respectively.

$$E_{hp_i} = E_{PV-hp_i} + E_{batt-hp_i} + E_{grid-hp_i} \quad (2)$$

The thermal power of the heat pump (P_{hp_i}, in kW_{th}) (to meet the demand load or store heat) must be lower or equal to the maximum thermal power output ($P_{hp-max-th_i}$ [kW_{th}]) at each time step (Eq. (3))

$$P_{hp_i} \leqslant P_{hp-max-th_i} \quad (3)$$

Eq. (4) defines the relationship between the electricity supply and heat generation, where E_{bu_i} [kWh_{el}] is the electricity consumption of the backup heater; $\dot{Q}_{hp-hs_i}$ [kWh_{th}] and $\dot{Q}_{hp-sh_i}$ [kWh_{th}] are the heat provided by the heat pump to the heat storage and directly to the space heating load, respectively. The COP, defined as the relationship between the heat flow (kW_{th}) provided by the heat pump, and its electrical power consumption (kW_{el}) (the COP is therefore dimensionless), is calculated at each time-step as a function of the outdoor temperature and the supply temperature using a lookup table from a recognized heat pump manufacturer (see Section 3 of the SI [48,49]).

$$E_{hp_i}\cdot COP_i + E_{bu_i} = \begin{cases} \dot{Q}_{hp-hs_i} \; if \; heat \; storage \\ \dot{Q}_{hp-sh_i} \; otherwise \end{cases} \quad (4)$$

Thermal mass and inertia of buildings can be substantial, e.g., allowing to keep the indoor temperature at comfort level for up to 6 h out of 24 h [33,50]. Thus, there is a delay between the thermal supply and demand as a function of outdoor temperature and thermal resistance [50]. Making use of the thermal inertia of buildings, the heat pump does not need to be perfectly aligned to heat demand as long as the total heat supplied within two hours matches the total demand within the same period [51]. Eq. (5) mathematically expresses the thermal inertia (or flexibility) of 2 h (8 blocks of 2 h represented by the sub-index j), where $\dot{Q}_{load_i}$ [kWh_{th}], $\dot{Q}_{hp-sh_i}$ [kWh_{th}] and $\dot{Q}_{ts-sh_i}$ [kWh_{th}]] are the space

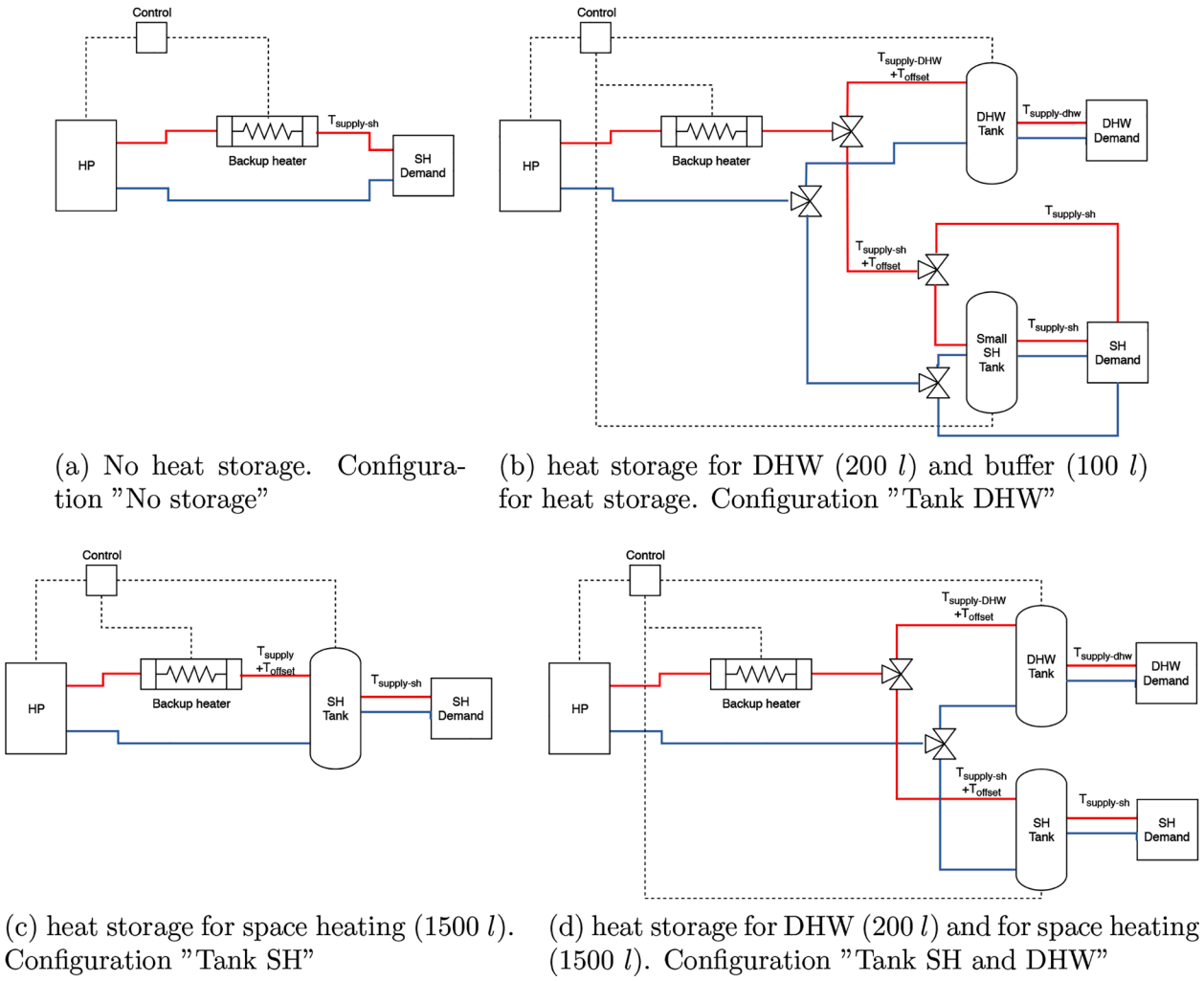

(a) No heat storage. Configuration "No storage"

(b) heat storage for DHW (200 l) and buffer (100 l) for heat storage. Configuration "Tank DHW"

(c) heat storage for space heating (1500 l). Configuration "Tank SH"

(d) heat storage for DHW (200 l) and for space heating (1500 l). Configuration "Tank SH and DHW"

Fig. 2. A schematic representation of the four heating system configurations used in this study, regardless of the use of battery storage.

heating demand, the heat supplied by the heat pump for space heating and the heat supplied by the heat storage for space heating, respectively.

$$\sum_{i=8\cdot j}^{8\cdot(j+1)} \dot{Q}_{load_i} = \begin{cases} \sum_{i=8\cdot j}^{8\cdot(j+1)} \dot{Q}_{ts-sh_i} & if \quad heat \quad storage \\ \sum_{i=8\cdot j}^{8\cdot(j+1)} \dot{Q}_{hp-sh_i} & otherwise \end{cases}$$
$$where\, j \in [0,7]\, and\, i \in [0,95] \tag{5}$$

3.2.2. Modeling of heat storage

Hot water tanks for space heating and DHW are modeled as perfectly mixed with a homogeneous temperature (T_{ts} [K]). Eqs. (6) and (7) present the change of heat content in the tanks as a function of time ($\Delta\dot{Q}_{ts_i}$ [kWh_{th}]) depending on the heat balance determined by the inlet flow from the heat pump ($\dot{Q}_{hp-hs}$), the heat flow delivered to the demand load ($\dot{Q}_{load}$ [kWh_{th}]), including both space heating and DHW, and the heat losses through the surface area to the surroundings ($\dot{Q}_{ts-loss}$ [kWh_{th}]). The amount of thermal energy charged into the heat storage (Q_{ts_i} [kWh_{th}]) is given in Eq. (8) by the difference between the temperature of the heat storage at time i (T_{ts_i} [K]) and the supply temperature (T_{supply_i} [K]), multiplied by the mass and the specific heat of water.

$$\Delta\dot{Q}_{ts_i} = \dot{Q}_{hp-hs_i} - \dot{Q}_{ts-sh_i} - \dot{Q}_{loss-ts_i} \tag{6}$$

$$\Delta\dot{Q}_{ts_i} = \left(T_{ts_i} - T_{ts_{i-1}}\right)\cdot m_{ts}\cdot c_{p_{ts}} \tag{7}$$

$$Q_{ts_i} = \left(T_{ts_i} - T_{supply_i}\right)\cdot m_{ts}\cdot c_{p_{ts}} \tag{8}$$

Moreover, hot water tanks for DHW and space heating operate between minimum (T_{supply_i} [K]) and maximum ($T_{supply_i}+T_{offset}$ [K]) temperature levels and they are characterized by losses ($Q_{loss-ts_i}$ [kWh_{th}]), as presented in Eqs. (9) and (10). Here, U_{ts} [$kW\cdot m^{-2}\cdot K^{-1}$], A_{ts} [m^{-2}] and ΔT_{ts_i} [K] are the heat storage's U-value, surface, and the difference of temperature (between the heat storage and the set-point temperature), respectively. The minimum temperature of the hot water tanks is constrained by the supply temperature (T_{supply} [K]; see Table 2). Furthermore, the maximum temperature is given by the supply temperature plus the offset temperature (i.e., ΔT [K]; see Table 2). It is assumed that the heat storage for space heating provides heat at the supply temperature (T_{supply} [K]), while the DHW tank, provides hot water at 50 °C.

$$T_{supply_i} \leqslant T_{ts} \leqslant T_{supply_i} + T_{offset} \tag{9}$$

$$\dot{Q}_{ts-loss_i} = U_{ts}\cdot A_{ts}\cdot \Delta T_{ts_i} \tag{10}$$

For DHW, the same equations as above apply, assuming a dedicated heat pump and a water tank of 200 l, according to the standard consumption of 50 l per person and per day for a single-family house, as defined in the Swiss norm SIA 385/2 [52]. For space heating, a 1500 l hot water tank is assumed for the SFH100. As for the SFH15 and SFH45,

Table 3
Various PV-coupled heat pump and storage configurations assessed in this study. Note that in all cases a 4.8 kW_p PV system is included and a heat pump of 4 kW_{th}, 6 kW_{th} or 16 kW_{th} provides space heating (and in some cases DHW) for the SFH15, SFH45 and SFH100, respectively. In the cases where DHW is not provided with a heat pump, an external fuel-based boiler is assumed (outside the scope of the model presented in this study).

Configuration	DHW provision with HP	Space heating tank size [l]	DHW tank size [l]	Corresponding heating system
No storage (Baseline scenario)	No	–	–	Fig. 2a
Tank DHW	Yes	100[a]	200	Fig. 2b
Tank SH	No	1500[b]	–	Fig. 2c
Tank SH and DHW	Yes	1500 b	200	Fig. 2d
Battery	No	–	–	Fig. 2a
Battery and Tank DHW	Yes	100 a	200	Fig. 2b
Battery and Tank SH	No	1500 b	–	Fig. 2c
Battery, Tank SH and DHW	Yes	1500 b	200	Fig. 2d

[a] Values for SFH15/SFH45/SFH100 respectively.
[b] SFH15 and SFH45 use the existing building storage (underfloor heating) which is considered equivalent to this size of water reservoir with a ΔT of 10 K. SFH100 uses a tank of the stated size for space heating.

underfloor heating allows to use the concrete of the floors and the heating water content as heat storage (i.e., existing building storage), thus, we do not consider any additional cost, since this feature is inherent to well insulated and retrofitted houses. This building storage is modeled as a tank of 1500 l with 10 K of ΔT (equivalent to a 9520 l water tank with 1.5 K of ΔT). The cost of the hot water tank for space heating is 66 USD/kWh (with a ΔT of 10 K) while for the DHW hot water tank the cost is 132 USD/kWh (with a ΔT of 20 K) [53]. Since the optimal storage size is mainly determined by the PV size [53], and since we pre-define the nominal PV capacity with the Swiss median for all scenarios and for all houses, no other tank sizes are considered. Furthermore, specific heat and U-values of 0.36 $W \cdot m^{-2} \cdot K^{-1}$ and 1.16 $Wh \cdot l^{-1} \cdot K^{-1}$ respectively are assumed for the tanks. The characteristics of the heat storage are shown in Table 2. In the cases where heat storage for space heating is not considered, a small buffer for space heating (100 l) is included regardless of the building type to ensure provision of both DHW and space heating (see Fig. 2b and d).

3.2.3. Electricity storage modeling and other constraints

Electricity storage with batteries is assumed to be integrated with the PV-coupled heat pumps using a DC–coupled topology since it is more affordable and efficient than AC–coupled topologies [54]. We use a 7 kWh_{el} NMC-based battery, which is the benchmark lithium-ion technology at the moment, with a pack cost of 335 USD/kWh_{el} of nominal capacity, 5000 cycles at 93% depth-of-discharge and a round-trip efficiency of 89% [55]. A maximum charge and discharge rates of 0.4 • C are assumed (i.e., the battery can be completely charged or discharged in 2.5 h). A bi-directional inverter is used to charge the battery from the grid and to exploit ToU tariffs and its cost is assumed to be 600 USD/kW_{el} [54]. In the cases without electricity storage, we consider a PV-inverter with a cost of 190 USD/kW_{el} [54].

The battery model, which includes ageing, and accounts for the electricity balance, the efficiency losses in the bi-directional inverter and power constraints for the battery, as well as the characteristics of the converter and the inverter, has been derived from a previous publication and presented in Section 4 of the SI [34]. Eq. (11) presents the constraint for demand peak-shaving, where P_{grid_i} [kWh_{el}] is the power drawn from or injected to the grid at any timestep and $P_{max-day}$ [USD/kWh_{el}] is the daily maximum power required from the grid. PS is the boolean flag indicating the presence of a capacity-based tariff (as in Eq. (1)).

$$P_{grid_i} \leqslant P_{max-day} \quad \forall \quad i \quad if \quad PS = True \tag{11}$$

3.2.4. System configurations

Eight PV-coupled heat pump configurations are compared in this study. In the baseline scenario, electricity and heat are provided using a PV-coupled heat pump without electricity or heat storage (see Fig. 2a). In this scenario, the existing storage of the SFH15 and SFH45 (i.e., the underfloor heating inherent to the house heating system), is disregarded to allow a direct comparison with the SFH100 (where the existing storage is very small, since it only consists of the radiators with a capacity below 100 l). In the configuration "Tank DHW" (see Fig. 2b), DHW is provided by the heat pump through a directly coupled tank while a small buffer for space heating is also considered (i.e., 100 l), in order to avoid the simultaneous use of the two virtual heat pumps (i.e., modeling purposes). For DHW provision without heat pumps, we assume another (non-electric) device, such as a gas boiler which is, however, not included in this analysis. In the configuration "Tank SH", heat storage for space heating is considered; for the SFH15 and SFH45 the underfloor heating is used as storage, whereas for the SFH100 a water tank with similar capacity is assumed (equivalent to 1500 l with 10 K ΔT, see Fig. 2c). A fourth configuration referred to as "Tank SH and DHW" includes DHW provision and heat storage for both space heating and DHW (see Fig. 2d). Furthermore, the same configurations including a battery are considered (see Table 3). In all cases, the space heating demand is provided in rather conservative blocks of 2 h (contrary to cases where higher blocks of flexibility are considered, e.g., [30,51,56,57]), giving an additional degree of flexibility to the system without compromising the thermal comfort. On the contrary, DHW is provided on-demand.

3.3. Distribution grid upgrading

The hosting capacity of distribution grids is being challenged by the addition of PV and heat pumps, together with electric vehicles. When this limit is reached, the distribution system needs to be upgraded. PV technology creates reverse power flow, potentially resulting in voltage violations and overloading of the distribution lines, while heat pumps increase the peak electricity demand [9]. The cost of distribution grid reinforcement depends on the location, e.g., the type of urban setting, for Switzerland, a recent study finds costs between 51–213 USD/kW_p for PV additions, and between 46–1385 USD/kW for heat pumps additions by 2035 [9]. Therefore, important investments are needed into distribution grids to enable the penetration of these technologies, which could be passed on to the consumers [58]. At high PV penetration, additional flexibility is required to supply PV electricity on-demand and keep the grid stability [58], with energy storage being a key flexibility provider as discussed in this study.

3.4. Techno-economic indicators

We use four important indicators to analyze trade-offs between prosumer benefits and grid impacts for the various system configurations: levelized cost, electricity peak flow, self-consumption rate and self-sufficiency rate. The levelized cost of meeting the electricity consumption, including the various energy services of the house, namely

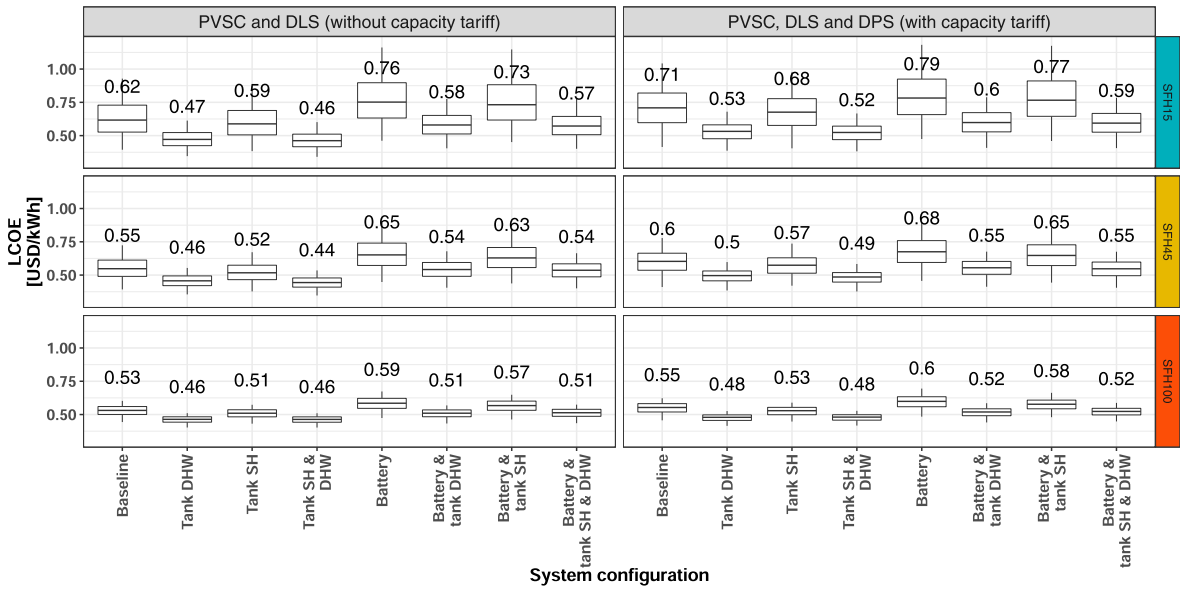

Fig. 3. Boxplots (N = 549) of the levelized cost of meeting the total electricity consumption, including space heating, hot water (if indicated) and all appliances, for all configurations depending on the combination of applications and the type of house. The line in the middle of the box and the number above the box represent the median LCOE. The box spans the first quartile to the third quartile, and the whiskers extend up to 1.5 times the interquartile range from the top or bottom of the box. PVSC stands for PV self-consumption, DLS for demand load shifting and DPS for demand peak shaving. Note that low values of LCOE are beneficial for the consumer.

space heating, hot water (if indicated) and all appliances, LCOE [USD/kWh_{el}]. It is calculated as shown in Eq. (12), as the sum of the CAPEX (including replacements) and operational expenditures (OPEX) considering the lifetime of the different technologies (PV, heat pump, tanks and battery), and divided by the total electricity demand $E_{total-demand}$, which encompasses the original electricity demand for appliances and lighting plus the heat pump electricity consumption [59]. A discount factor, r, is used to account for the time value of money, the risk associated with the project and the inflation.

$$LCOE = \frac{\sum_{i=0}^{N} \frac{CAPEX}{(1+r)^i} + \sum_{i=1}^{N} \frac{OPEX}{(1+r)^i}}{\sum_{i=1}^{N} \frac{E_{total-demand}}{(1+r)^i}} \quad (12)$$

The different cost of constructing the buildings (SFH15, SFH45 and SFH100) or of retrofitting them to the corresponding thermal characteristics are not considered. For prosumers, we also use as indicators the self-consumption (SC), which is the share of on-site PV generation that is used to cover the local electricity demand (including the heat pump) and self-sufficiency (SS), which is the share of local demand (including appliances, lighting, and heat pump) that is covered by the on-site PV generation as shown in Eqs. (13) and (14).

$$SC = \frac{\sum_{i=0}^{N} \left(E_{PV-total-demand} + E_{PV-batt}\right)}{\sum_{i=0}^{N} E_{PV}} \quad (13)$$

$$SS = \frac{\sum_{i=0}^{N} \left(E_{PV-total-demand} + E_{batt-load}\right)}{\sum_{i=0}^{N} E_{total-demand}} \quad (14)$$

Here N refers to the system lifetime (30 y); $E_{PV-total-demand}$ is the share of PV generation that directly meets local electricity demand; $E_{PV-batt}$ is the share of PV generation that is charged into the battery; E_{PV} is the total PV generation; and $E_{batt-load}$ is the amount of electricity discharged from the battery to cover local electricity demand. We graphically visualize these two indicators in an energy matching chart, which is a type of graph that shows the matching between PV generation and demand for different types of buildings (see Fig. 5) [60]. To analyze grid impacts, we finally consider the peak power flow which is defined as the maximum between imports from and exports to the grid [28].

4. Results

We present the results in three steps as a function of the thermal characteristics of the houses. Every building type (i.e., SFH15, SFH45 and SFH100), was matched with 549 electricity profiles (i.e., a total of 1647 profiles). Then, the optimization was run throughout a full-year and the results were scaled over a time period of 30 yr corresponding to the lifetime of the PV system. First, we display boxplots comparing LCOE and peak flows per building type for each configuration with and without demand peak shaving (i.e., with and without the inclusion of a capacity-based tariff). Secondly, we display an energy matching chart to analyze self-consumption (SC) and self-sufficiency (SS) depending on the type of storage, namely batteries and hot water tanks (with and without DHW provision). Likewise, the LCOEs and peak flows are plotted in order to get an understanding of the trade-offs between prosumer benefits and grid impacts. To highlight statistically significant differences across the results, we perform a Shapiro–Wilk test to prove non-normality of the results [61], followed by a paired Wilcoxon test with Holm procedure to control the family-wise error rate, to determine if two or more sets of pairs are different from one another in a statistically significant manner [62]. All tests results are presented in Section 9 of the SI. The statistical analyses were performed in R (R Core Team) [63]. We use kW_{el} and kW_{th} to refer to electricity and heat respectively.

4.1. LCOE

Fig. 3 displays the levelized cost of meeting the total electricity consumption for the three building types and eight configurations. Four major observations can be made. First, the LCOE of SFH15 (which corresponds to the Swiss Minergie-P or German Passivhaus) are significantly higher ($p-values \leqslant 0.001$) than for SFH45 (modern building from the years 2000–2010) or SFH100 (renovated building from before 1980 or a building from 1980–1990), in particular, when DHW provision is not considered. For example, the difference between the median values of SFH15 and SFH100 reaches 0.17 USD/kWh_{el} for a PV-coupled heat pump connected to a battery and in the presence of a capacity-based tariff. The reason for these differences is twofold, on one hand the specific CAPEX and on the other hand, the electricity consumption of the heat pumps leads to very different electricity demand depending on the

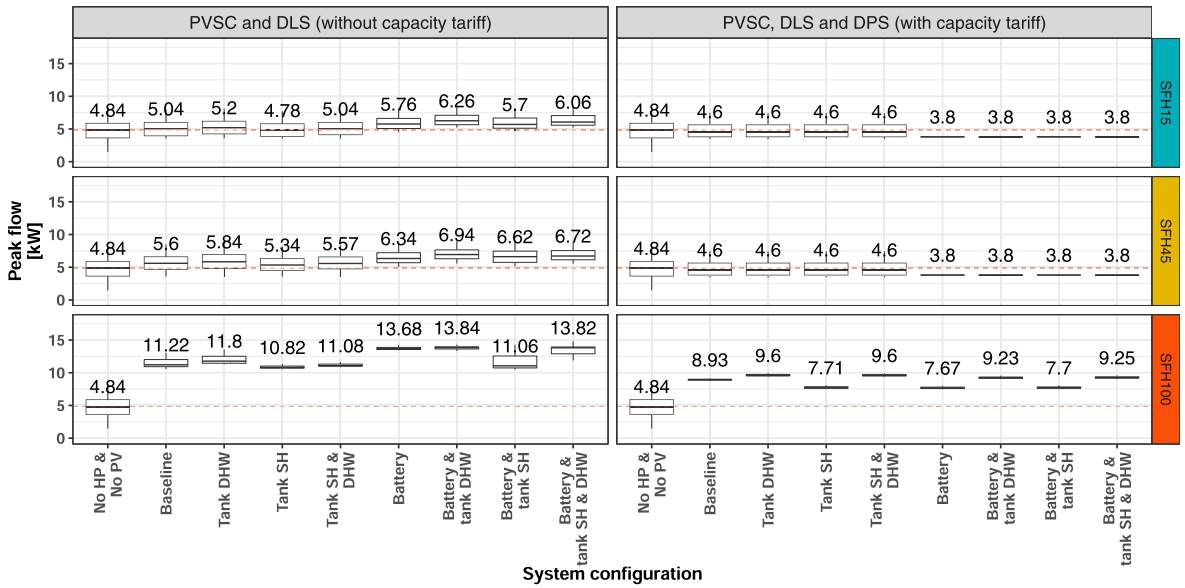

Fig. 4. Boxplots (N = 549) of the peak flow defined as the maximum peak power, considering import from and export to the grid, for all configurations depending number of storage applications (PVSC is PV self-consumption, DLS is demand load-shifting and DPS is demand peak-shaving with a capacity-based tariff) and the type of house (SFH15, SFH45 and SFH100). For comparison, the original electricity load, without PV generation or heat pump is also displayed (No HP & No PV). The line in the middle of the box and the number above the box represent the median peak flow. The box spans the first quartile to the third quartile, and the whiskers extend up to 1.5 times the interquartile range from the top or bottom of the box. The dashed red line represent the median of the classic electricity load distribution.

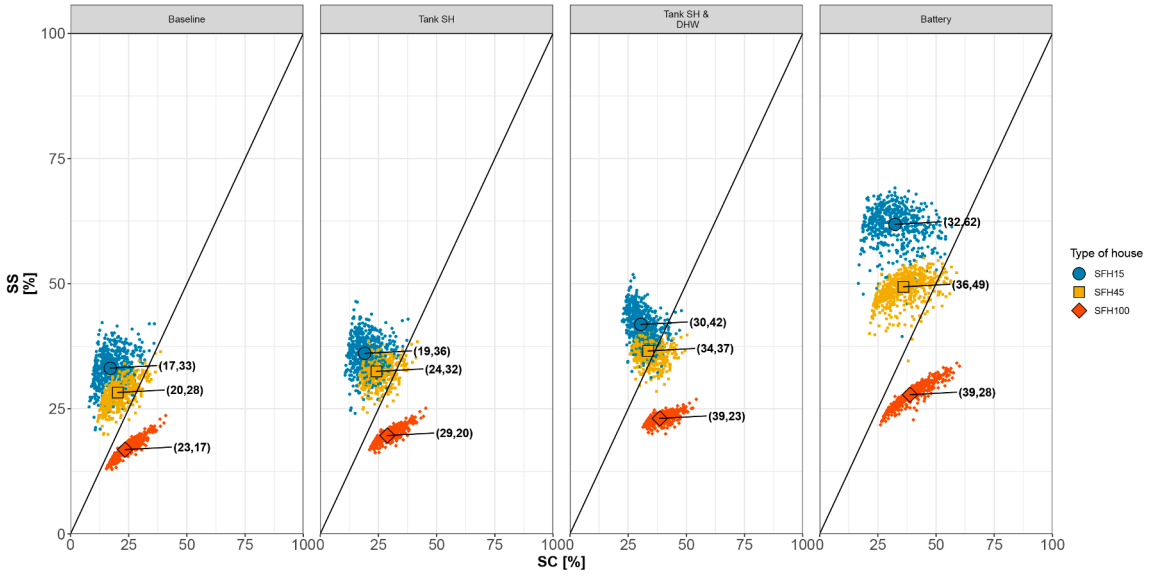

Fig. 5. Energy matching chart to analyze self-consumption (SC) and self-sufficiency (SS) for a PV-coupled heat pumps as a function of the type of storage, namely, none (baseline case), heat storage for space heating alone, heat storage for space heating and with DHW and finally, with only a battery. The configurations presented here include a capacity-based tariff in the electricity tariff. The big black circle, square and diamond represent the median by type of house.

thermal envelope of the building, with medians of 8120 kWh_{el}, 3420 kWh_{el} and 2260 kWh_{el} p.a. for the SFH100, SFH45 and SFH15, respectively (see Section 7 of the SI). Secondly, DHW provision, which accounts for around 1300 kWh_{el} p.a. of heat pump electricity consumption, reduces significantly the LCOE ($p-values \leqslant 0.001$) regardless of the type of house. Furthermore, the better the thermal insulation of the house, the higher the impact of DHW on the LCOE. For instance, the median LCOE value is reduced by 0.05 USD/kWh_{el}, 0.11 USD/kWh_{el} and 0.17 USD/kWh_{el} for a PV-coupled heat pumps assisted with thermal storage for space heating and DHW in SFH100, SFH45 and SFH15, respectively, compared to the baseline (without storage).

Thirdly, the use of batteries significantly increases the median LCOE values by up to 0.08 USD/kWh_{el} relative to the baseline ($p-values \leqslant 0.001$), mainly as a consequence of the CAPEX of the battery. Finally, the inclusion of a capacity component in the retail tariff (to enable demand peak shaving) entails a significant increase of the LCOE ($p-values \leqslant 0.001$) for houses with high thermal standard due to the lower impact of the volumetric component of the electricity tariff on the costs. The median increases of LCOE values due capacity-based tariffs are 0.05 USD/kWh_{el}, 0.03 USD/kWh_{el} and 0.01 USD/kWh_{el} for SFH15, SFH45 and SFH100, respectively.

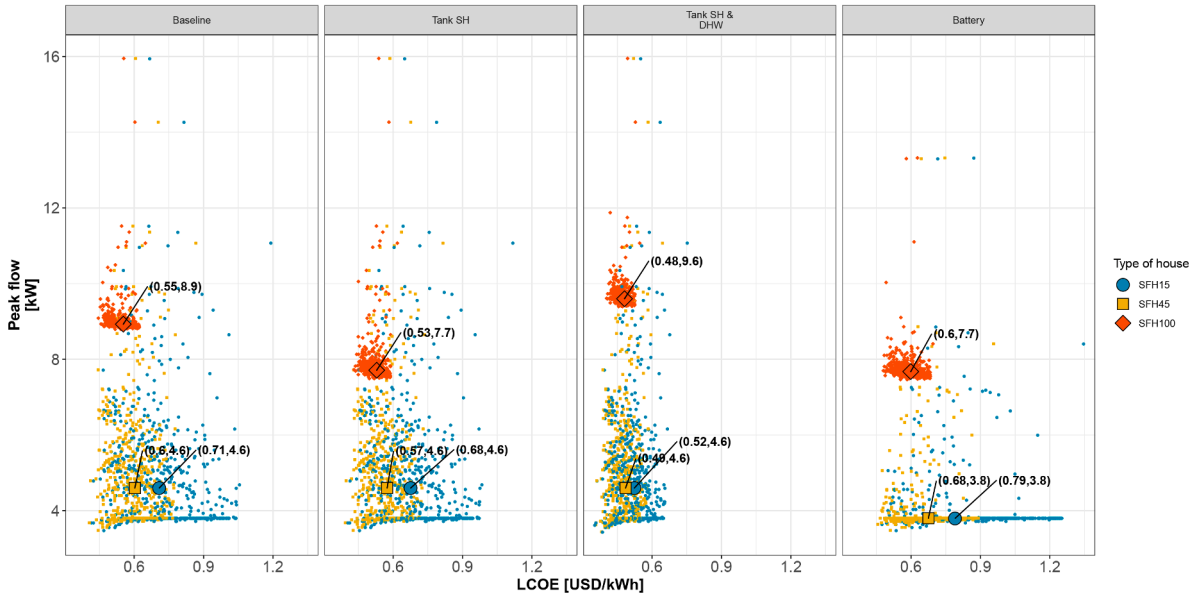

Fig. 6. LCOE vs peak flow for a PV-coupled heat pumps as a function of the type of storage, namely, none (the baseline case), heat storage for space heating alone, heat storage for space heating and with DHW and finally, with only a battery. The configurations presented here include a capacity-based tariff in the electricity tariff. The big black circle, square and diamond represent the median by type of house.

4.2. Peak flow

Fig. 4 displays the peak flow depending on the system configuration and the type of house. Three major observations can be made. First, the peak flow is significantly higher ($p-values \leqslant 0.001$) in houses with poor thermal envelope (SFH100), compared to houses with high (SFH45) and very high thermal performance (SFH15), which is a direct result of the heat pump capacity. For instance, the median of the peak flows across all configurations for SFH100 with (without) the capacity-based tariff are 9.1 kW_{el} (12.1 kW_{el}), 5.3 kW_{el} (6.5 kW_{el}) more than for SFH15.

Secondly, heat pump operation has only a rather small impact on the peak flow of SFH15 and SFH45, thanks to their envelope quality. Heat pumps only have a peak power of 1.7 kW_{el} and 2 kW_{el} respectively, which is lower than the median peak of the original demand for appliances and lighting (4.8 kW_{el}, see the case "No HP & no PV" in Fig. 4). Furthermore, the peaks of the original demand and the heat pump are not simultaneous. In contrast, for renovated old houses (SFH100), the heat pump peak power (6.6 kW_{el}) strongly impacts the peak flow, doubling the original demand for appliances and lighting.

Fig. 4 also shows that the impact of the type of storage depends on the thermal characteristics of the house and the presence of a capacity-based tariff. Batteries slightly reduce (increase) the peak flow by 0.8 kW_{el} (1.3 kW_{el}), depending on whether a capacity-based tariff is in place or not (this result is statistically significant, with $p-values \leqslant 0.001$). In poorly insulated houses, heat storage slightly reduces (increases) the peak flow by 1.2 kW_{el} (0.7 kW_{el}) depending on the capacity-based tariff. With batteries as energy storage, the peak flow of PV-coupled heat pumps varies very strongly depending on whether the electricity tariff includes or not a capacity-based tariff, decreasing by 1.2 kW_{el} and increasing by 2.6 kW_{el} respectively, regarding the base case (no storage), with differences being statistically significant, with $p-values \leqslant 0.001$ in both cases.

4.3. Graphical comparison electricity and heat storage

We compare electricity and heat storage, first in terms of self-consumption and self-sufficiency (Fig. 5), and secondly in terms of LCOE and peak flow (Fig. 6), assuming that a capacity-based tariff is included in the electricity tariff.

Fig. 5 shows a limited increase in the median values of self-consumption (2–6%) and self-sufficiency (3–4%) for the inclusion of a hot water tank for space heating only (represented with a black circle, square and diamond according to the type of house) for the three types of house (despite being statistically significant, with $p-values \leqslant 0.001$). When a heat pump is used to provide both space heating and DHW, the increase in self-consumption is high (13–16%) and moderate for self-sufficiency 6–9%) (values are statistically significant, with $p-values \leqslant 0.001$). On the other hand, adding a battery to the PV-coupled heat pumps leads to important increases in self-consumption (15–16%) and self-sufficiency (11–29%), for the three types of house (statistically significant, with $p-values \leqslant 0.001$). Values for other configurations are shown in the SI Section 8, and similar patterns can be observed.

Fig. 6 shows a graphical comparison of the LCOE and the peak flow by type of house for the different types of storage added to the PV-coupled heat pumps. The inclusion of heat storage for space heating marginally reduces the LCOE for SHF15, SFH45 and SFH100 by 0.03 USD/kWh_{el}, 0.03 USD/kWh_{el} and 0.02 USD/kWh_{el}, respectively ($p-values \leqslant 0.001$). More importantly, heat storage allows to maintain the peak flow at the same levels as the baseline case and even helps to reduce it by 1.2 kW_{el} in inefficient houses (SFH100). When DHW is added as demand load, the LCOE decreases further by 0.16 USD/kWh_{el}, 0.08 USD/kWh_{el} and 0.07 USD/kWh_{el} for SHF15, SFH45 and SFH100, respectively. However, the median peak flow in the older house is pushed to 9.6 kW_{el} above the baseline median value (which excludes DHW, see Table 3), while in the more efficient houses the median peak flow remains at the same level.

On the other hand, the addition of a battery leads to an increase of the median LCOE between 0.04–0.08 USD/kWh_{el} depending on the type of house (statistically significant, $p-values \leqslant 0.001$). However, a battery decreases the peak flow if a capacity-based tariff is present, with a median peak reduction between 0.8–1.2 kW_{el} depending on the type of house ($p-values \leqslant 0.001$).

5. Discussion

Our results highlight some of the challenges, and opportunities associated with the decarbonization of the heating sector in the context of decarbonization. First, installing heat pumps without retrofitting the thermal envelope markedly increases (up to twice) the peak flow in poorly insulated houses (i.e., SFH100). This increase is a direct consequence of the size of the heat pump required to supply the heat demand. Furthermore, the provision of DHW using heat pumps and electric backup heaters entails even a higher peak flow in poorly insulated houses. Consequently, thermal retrofitting does not only help to reduce carbon dioxide emissions and to increase comfort levels [2,64], but also to reduce grid stress.

Thermal retrofitting would reduce investments on distribution grid upgrading due to PV and heat pump penetration. In Switzerland, indicative costs of grid upgrading under a conservative scenario of PV penetration (4.2 GW_p) reach up to 0.49 billion USD, while they amount to 0.78 billion USD for 6.4 GW_{el} of installed heat pump capacity [9]. However, two main obstacles have to be overcome. First, the low retrofitting rate of 1% p.a. has to be increased. Secondly, a large investment is also needed for energy retrofitting. For instance, retrofitting houses which are originally not well insulated (SFH100) to very high insulation standards (SFH15) costs around 730 USD/m^2 [65,2], i.e. 100.000 USD for a standard single-family house of 140 m^2 as considered in this study. Overall, the cost to improve the thermal performance of all the SFH in Switzerland is around 35 billion USD [66]. These are very high values for the house owners and may be subject of subsidies from the government, but interestingly, an economic saving potential of more than 50% for the Swiss residential building stock has been proved [65]. Nevertheless, the extent of the economic saving potential for the distribution grid (avoidance of grid upgrade) remains an open question, which should be subject of future work.

We find that the implementation and design of capacity-based tariffs are fundamental to limit the grid impacts associated with the performance of PV and heat pumps, as well as batteries charging from the grid (i.e., performing demand load shifting). Capacity-based tariffs provide price signals for prosumers to reduce their peak flow, which can help to defer distribution grid upgrades and to recover a portion of network costs [45]. On the other hand, policy makers and regulators need to carefully design such capacity-based tariffs in order to avoid costly household bill expenditures [45]. We acknowledge that although capacity-based tariffs have been widely applied for large consumers, their application has so far been more limited for residential customers. However, there are some first pilot projects and demonstrations, e.g., in the Netherlands, France, Italy Finland and Spain [67–69]. Their implementation for residential consumers is now being suggested following the penetration of PV, air conditioning, heat pumps and electric vehicles. As shown in this study, the performance of these various technologies modify the electricity demand profile and in particular, increase the peak demand, which may lead to to voltage issues, and overloading of lines and transformers [70–72].

It is important to highlight that energy storage can be a two-edged sword, reducing or increasing the peak flow depending whether a capacity-based tariff is present or not. When capacity-based tariffs are included, batteries allow to reduce the peak flow, even below the case without neither PV nor heat pump, in houses which are well and very well insulated. In houses which are poorly insulated, batteries also reduce the peak flow below the baseline scenario (i.e., without storage) as long as DHW is not met using electricity (i.e., an additional non-electric heat generator is used to meet DHW). Our results show a similar pattern for heat storage for space heating, however, heat storage reduces the peak flow less markedly, even with high capacity-based tariffs (see SI Section 10). The beneficial effect of heat storage could be increased by increasing the offset temperature and/or by allowing further flexibility, beyond the two hours-blocks assumed in this study. However,larger tanks, under the same conditions (PV size of 4.8 kW_p, two hours-blocks and 10 K of temperature difference) would only increase self-consumption and self-sufficiency by 1 percent point, while the peak flow remains steady and the LCOE increases by 0.01 USD/kWh_{el} (see SI Section 7). The peak flow is mainly determined by the PV export in well insulated houses, whereas the peak demand is predominant in poorly insulated houses. This explains why the peak flow in well insulated houses is not reduced below the threshold determined by the PV nominal capacity unless PV curtailment is implemented.

The supply of DHW by heat pumps (around 1300 kWh_{el} p.a.) is highly beneficial for an investment of a PV-coupled heat pumps since it considerably reduces the LCOE (up to 0.17 USD/kWh_{el}) and increases the self-consumption rate by more than 10%, while incurring in a relatively small extra capital investment (960 USD). Conversely, DHW supply implies an increased peak flow in poorly insulated houses (SFH100). As an important finding, the use of batteries enables a significant increase in self-sufficiency and self-consumption, by up to 16% and 29%, respectively. However, the still high cost of batteries increases the LCOE markedly (up by 0.08 USD/kWh_{el}). Thus, battery cost reduction is urgently needed to pave the way towards win–win situations for prosumers and the grid, in particular for well insulated houses. Finally, access to low financing costs (i.e., reflected by the discount factor) is key to reduce the burden on prosumers who invest on low carbon technologies to decarbonize the heating sector, followed by subsidies to reduce the upfront cost of carbon-free technologies.

Our study proposes a robust framework to quantify the impacts of storage technologies on PV-coupled heat pumps and the proposed model is rich in technology details. However, it is not without limitations, which in turn call for future research. Our methodological approach includes some simplifications such as the assumption of a steady state of the buildings' thermal performance and of perfectly-mixed water tanks. More detailed thermal modeling of both buildings and hot water tanks would have increased the computation time markedly. Daily schedule optimization could restrict heat storage flexibility and its economic case, but on the other hand, a longer optimization windows increases the forecast uncertainty, in particular of demand peaks. Forecast strategies (perfect forecast is assumed in this study), together with alternative optimization windows (midnight to midnight is assumed in this study) may cut down the peak flow reductions and increase LCOE values. We assume a rather limited thermal inertia of buildings implying that the heat supply must match the heat demand every 2 h . In contrast, more flexible hot water tanks (larger size, higher temperature levels and stratification) and houses could boost the role of heat storage. However, we argue that extra thermal inertia and its associated flexibility (e.g., 24

h) may not be representative for the entire building stock, in particular for houses with poor envelope quality, calling for further empirical evidence. In addition, we use a representative size of energy storage (both electricity and heat) for comparability reasons, whereas alternative sizes may modify the trade-offs between prosumer benefits and grid impacts (inclusion of sizing in the optimization could hence lead to different findings). Importantly, the design of future electricity tariffs including ToU and capacity-based components calls for further interdisciplinary research to tackle energy justice [45]. Future research can also include electric vehicles and use our open-source optimization model with different locations with temperate climate and fast diffusion of PV and heat pumps.

6. Conclusions and policy implications

This study analyzes the trade-offs between prosumer benefits and grid impacts for PV-coupled heat pumps, providing space heating and domestic hot water for residential buildings characterized by different thermal performance. We also compare electricity and heat storage based on existing time-of-use tariffs and capacity-based tariffs.

Importantly, we find that energy retrofitting is very effective (up to 50% smaller peak flow in well insulated buildings) for decreasing the grid impacts of heating electrification. Consequently, policy measures incentivizing building retrofitting are beneficial not only for the owners and tenants, in terms of improved thermal comfort and lower heating bills, but also for distribution grid operators that may defer (or completely avoid) upgrades. Secondly, we recommend the following steps to increase the share of PV self-consumption and self-sufficiency, based on our techno-economic results, in houses with a PV-coupled heat pumps: first, to supply domestic hot water; secondly to install heat storage; and lastly, to use a battery.

Thirdly, the implementation and design of capacity-based tariffs are fundamental to relieve grid impacts from PV, batteries and electric heating with heat pumps. Based on our results, we conclude that heat storage reduces the levelized cost of meeting the electricity consumption, in particular when heat pumps are used for space heating and DHW, while it allows high self-consumption (30–39% comparable with batteries). On the other hand, both heat storage and batteries are found to be a two-edge sword, since they can either increase or decrease the peak demand depending on the presence of capacity-based tariffs. Based on representative sizes (i.e., 7 kWh_{el} battery and 1500 l hot water tank), we conclude that batteries are more effective than heat storage in increasing the self-sufficiency of houses with PV-coupled heat pumps.

However, decarbonizing heating demand using local PV supply enabled by storage is still costly (i.e., the cost of meeting the electricity related to the various energy services of the house, including space heating, hot water and all appliances is in the range of 0.55–0.71 USD/kWh_{el}) and therefore, appropriate policy incentives are needed. In order to be economically efficient, research and innovation policy should be designed in a way that reduces societal cost. Based on our analysis, we recommend that policy should support research and incentives on levers which simultaneously maximize prosumer benefits and minimize their grid impacts, such as building energy retrofitting, energy storage and capacity-based tariffs.

CRediT authorship contribution statement

Alejandro Pena-Bello: Conceptualization, Investigation, Methodology, Software, Formal analysis, Validation, Writing - original draft. **Philipp Schuetz:** Methodology, Software, Validation, Writing - review & editing. **Matthias Berger:** Writing - review & editing. **Jörg Worlitschek:** Writing - review & editing. **Martin K. Patel:** Writing - review & editing, Supervision. **David Parra:** Conceptualization, Methodology, Software, Validation, Writing - review & editing, Supervision, Project administration, Funding acquisition.

Declaration of Competing Interest

The authors declare that they have no known competing financial interests or personal relationships that could have appeared to influence the work reported in this paper.

Acknowledgements

This research project was financially supported by the Swiss Innovation Agency Innosuisse and is part of the Swiss Competence Center for heat and electricity Storage (SCCER-HaE), while also contributing to the Competence Center for Research in Energy, Society and Transition (CREST) as well as to the Swiss Competence Center for Energy Research on Future Energy Efficient Buildings & Districts (SCCER FEEB&D). The research for the calculation tool of the building heating load was funded by the European Commission, H2020-project Heat4Cool, Grant No. 723925 as well as by the Swiss State Secretariat for Education, Research and Innovation (SERI) under Contract No. 16.0082. Furthermore, we thank Pablo Timoner for his insights in statistical significance.

Appendix A

Table A.1
Values selected for the technical and economic assessment of PV-coupled heat pumps supported by electricity and heat storage.

Component	Units	Value	Reference
PV size	[kW]	4.8	
PV lifetime	[years]	30	[46]
PV module cost	[USD/kW]	1032	[46]
PV Balance of plant cost	[USD/kW]	240	[46]
PV Installation costs (labour costs)	[USD/kW]	514	[46]
PV Installation costs (other costs)	[USD/kW]	163.5	[46]
PV O&M	[USD/kW]	103	[46]
PV inverter cost	[USD/kW]	190	[73]
PV inverter lifetime	years	15	[73]
Inverter efficiency	%	94	[17]
ILR	p.u.	1.2	[74]
Charge controller efficiency	%	98	[17]
Bi-directional inverter cost	[USD/kW]	600	[54]
Bi-directional inverter lifetime	years	15	[73]
Battery pack cost	[USD/kWh_{el}]	335	[55]
Battery balance of plant cost	[USD]	2000	[75]
Battery O&M	[USD/kW]	0	[55]
Battery round-trip efficiency	%	89	[55]
End of life (EoL)	%	70	[17]
HP lifetime	[years]	20	[53]
HP module cost	[USD/kW]	1650	[53]
HP Installation costs	[USD/kW]	2200	[53]
HP O&M	% of CAPEX p.a.	1.1	[53]
Hot water tank lifetime	[years]	20	[53]
Hot water tank cost @ 10 K ΔT	[USD/kWh_{th}]	66	[53]
Hot water tank cost @ 20 K ΔT	[USD/kWh_{th}]	132	[53]
Hot water tank Installation costs	[USD/kWh_{th}]	0	[53]
Hot water tank O&M	[USD/kWh_{th}]	0	[53]
Discount factor	%/a	4	[17]
EUR to USD rate	p.u.	1.1	

Table A.2
List of model parameters and variables.

Modeling parameters	Name	Units	Modeling variables	Name	Units
Converter efficiency	η_{conv}	%	PV generation fed to the load	$E_{PV-load}$	kWh_{el}
Inverter efficiency	η_{inv}	%	PV generation exported to the grid	$E_{PV-grid}$	kWh_{el}
Inverter rating	P_{inv}	kW	PV generation injected to the battery	$E_{PV-batt}$	kWh_{el}
Battery Efficiency	η_{batt}	%	PV generation curtailed	$E_{PV-curt}$	kWh_{el}
Maximum discharge power	$P_{max-dis}$	kW	Energy lost due to converter efficiency	$E_{loss-conv}$	kWh_{el}
Maximum charge power	$P_{max-char}$	kW	Total energy lost due to bi-directional inverter efficiency	$E_{loss-binv}$	kWh_{el}
Battery nominal capacity	C_{batt}^{nom}	kWh_{el}	PV energy lost due to bi-directional inverter efficiency	$E_{loss-PVinv}$	kWh_{el}
Battery lifetime	N	years	Grid energy lost due to bi-directional inverter efficiency	$E_{loss-gridinv}$	kWh_{el}
Battery maximum state of charge	SOC_{max}	%	Battery energy lost due to bi-directional inverter efficiency	$E_{loss-battinv}$	kWh_{el}
Battery minimum state of charge	SOC_{min}	%	Energy lost due to battery efficiency	$E_{loss-batt}$	kWh_{el}
Retail prices	π_{import}	USD/kWh_{el}	Energy drained from the battery	E_{dis}	kWh_{el}
Export prices	π_{export}	USD/kWh_{el}	Energy injected to the battery	E_{char}	kWh_{el}
Capacity tariff	$\pi_{capacity}$	USD/kW	Energy delivered from the battery to the load	$E_{batt-load}$	kWh_{el}
Feed-in limit	P_{limit}	%	Energy imported from the grid to the battery	$E_{grid-batt}$	kWh_{el}
Combination of applications	[PVCT, PVSC, DLS, DPS]	Boolean array	Energy imported from the grid to the load	$E_{grid-load}$	kWh_{el}
Load demand	E_{load}	kWh_{el}	Energy drained from the grid	E_{grid}	kWh_{el}
PV generation	E_{PV}	kWh_{el}	State of charge	SOC_i	%
Space heat demand (SH)	Q_{load}	kWh_{th}	PV generation fed to the HP for SH	E_{PV-hp}	kWh_{el}
Domestic heat water demand	Q_{dhw}	kWh_{th}	PV generation fed to the HP for DHW	E_{PV-hpw}	kWh_{el}
Nominal power of the HP	$P_{HP_{nom}}$	kW	Energy from the battery fed to the HP for SH	$E_{batt-hp}$	kWh_{el}
Coefficient of Performance	COP_i	-	Energy from the battery fed to the HP for DHW	$E_{batt-hpw}$	kWh_{el}
Temperature minimum of SH tank	$T_{ts_{min}}$	K	Energy from the grid fed to the HP for SH	$E_{grid-hp}$	kWh_{el}
Temperature maximum of SH tank	$T_{ts_{max}}$	K	Energy from the grid fed to the HP for DHW	$E_{grid-hpw}$	kWh_{el}
Temperature minimum of DHW tank	$T_{tsw_{min}}$	K	Thermal energy in the SH tank	Q_{ts}	kWh_{th}
Temperature maximum of DHW tank	$T_{tsw_{max}}$	K	Thermal energy in the DHW tank	Q_{tsw}	kWh_{th}
U-value SH tank	U_{ts}	$kW*m^{--2}*K^{--1}$	Thermal energy lost in the SH tank	$Q_{losses_{ts}}$	kWh_{th}
U-value DHW tank	U_{tsw}	$kW*m^{--2}*K^{--1}$	Thermal energy lost in the DHW tank	$Q_{losses_{tsw}}$	kWh_{th}
Surface SH tank	A_{ts}	m^2	Thermal energy flow from SH tank to SH	Q_{ts-sh}	kWh_{th}
Surface DHW tank	A_{tsw}	m^2	Thermal energy flow from DHW tank to DHW	$Q_{tsw-dhw}$	kWh_{th}
Specific heat SH tank fluid	$c_{p_{ts}}$	$kWh*kg^{--1}*K^{--1}$	Thermal energy supplied by the HP to the SH tank	Q_{hp-ts}	kWh_{th}
Specific heat DHW tank fluid	$c_{c_{tsw}}$	$kWh*kg^{--1}*K^{--1}$	Thermal energy supplied by the HP to the DHW tank	$Q_{hpw-tsw}$	kWh_{th}
Mass SH tank fluid	m_{ts}	kg	Thermal energy supplied by the HP SH demand	Q_{hp-sh}	kWh_{th}
Mass SH tank fluid	m_{tsw}	kg	Temperature of the SH tank	T_{ts}	K
Configuration	[Batt, heating, ts, DHW]	Boolean array	Temperature of the DHW tank	T_{ts}	K
Optimization time framework t	minutes	-	Maximum power drained from the grid	$P_{max-day}$	kW
Temporal resolution	Δt	fraction of hour	Power related to any energy parameter	$P_x = E_x/\Delta t$	kW

Appendix B. Supplementary data

Supplementary data associated with this article can be found, in the online version, at https://doi.org/10.1016/j.enconman.2021.114220.

References

[1] IEA. REnewables 2020; 2020. (Accessed on 12/01/2021). Available from: https://www.iea.org/reports/renewables-2020.

[2] Streicher KN, Padey P, Parra D, Bürer MC, Schneider S, Patel MK. Analysis of space heating demand in the Swiss residential building stock: Element-based bottom-up model of archetype buildings. Energy Build 2019;184:300–22 (Accessed on 12/01/2021).

[3] Staffell I, Brett D, Brandon N, Hawkes A. A review of domestic heat pumps. Energy Environ Sci 2012;5(11):9291–306. https://doi.org/10.1039/C2EE22653G (Accessed on 12/01/2021). Available from:.

[4] Dott R, Ackerman C, Koch M, Afjei T, Eismann R. Wärmepumpenheizsysteme mit PV und weiteren Komponenten; 2019. [Accessed on 12/01/2021]. Available from: https://www.fws.ch/wp-content/uploads/2019/05/Ralf_Dott.pdf.

[5] Castelazzi L, Zangheri P, Paci D, Economidou M, Labanca N, Ribeiro Serrenho T, et al. Assessment of second long-term renovation strategies under the Energy Efficiency Directive. JRC Science for Policy Report JRC114200 2019.

[6] Rinaldi A, Soini MC, Streicher K, Patel MK, Parra D. Decarbonising heat with optimal PV and storage investments: A detailed sector coupling modelling framework with flexible heat pump operation. Appl Energy 2020;282:116110.

[7] Barbour E, González MC. Projecting battery adoption in the prosumer era. Appl Energy 2018;215:356–70. https://doi.org/10.1016/j.apenergy.2018.01.056 [Accessed on 12/01/2021]. Available from:.

[8] Wang Z. Optimizing the Grid Integration of Distributed Solar Energy [PhD dissertation]. Virginia Commonwealth University. Virginia Commonwealth University; 2018. [Accessed on 12/01/2021] https://pdfs.semanticscholar.org/9093/69cd437ec5573aed35f956b6fa3f5f8c44cb.pdf.

[9] Gupta R, Pena-Bello A, Streicher KN, Roduner C, Thöni D, Patel MK, et al. Spatial analysis of distribution grid capacity and costs to enable massive deployment of PV, electric mobility and electric heating. Appl Energy 2021;287:116504.

[10] Sichilalu SM, Xia X. Optimal power dispatch of a grid tied-battery-photovoltaic system supplying heat pump water heaters. Energy Conver Manag 2015;102:81–91.

[11] Lund PD, Lindgren J, Mikkola J, Salpakari J. Review of energy system flexibility measures to enable high levels of variable renewable electricity. Renew Sustain Energy Rev 2015;45:785–807.

[12] Salpakari J, Lund P. Optimal and rule-based control strategies for energy flexibility in buildings with PV. Appl Energy 2016;161:425–36.

[13] IEA. Tracking Buildings; 2019. (Accessed on 12/01/2021). Available from: https://www.iea.org/reports/tracking-buildings.

[14] Parra D, Walker GS, Gillott M. Are batteries the optimum PV-coupled energy storage for dwellings? Techno-economic comparison with hot water tanks in the UK. Energy Build 2016;116:614–21.

[15] Luthander R, Widen J, Munkhammar J, Lingfors D. Self-consumption enhancement and peak shaving of residential photovoltaics using storage and curtailment. Energy 2016;Oct: 112. [Accessed on 12/01/2021]. Available from: doi: 10.1016/j.energy.2016.06.039.

[16] Campana PE, Cioccolanti L, François B, Jurasz J, Zhang Y, Varini M, et al. Li-ion batteries for peak shaving, price arbitrage, and photovoltaic self-consumption in commercial buildings: A Monte Carlo Analysis. Energy Convers Manag 2021;234:113889.

[17] Pena-Bello A, Barbour E, Gonzalez MC, Yilmaz S, Patel MK, Parra D. How does the electricity demand profile impact the attractiveness of PV-coupled battery systems combining applications? Energies 2020;13(15):4038.

[18] Heymann F, Silva J, Miranda V, Melo J, Soares FJ, Padilha-Feltrin A. Distribution network planning considering technology diffusion dynamics and spatial net-load behavior. Int J Electr Power Energy Syst 2019;106:254–65. https://doi.org/10.1016/j.ijepes.2018.10.006 [Accessed on 12/01/2021]. Available from:.

[19] Patteeuw D, Henze GP, Helsen L. Comparison of load shifting incentives for low-energy buildings with heat pumps to attain grid flexibility benefits. Appl Energy 2016;167(80–92). https://doi.org/10.1016/j.apenergy.2016.01.036 [Accessed on 12/01/2021]. Available from:.

[20] Verhelst C, Logist F, Van Impe J, Helsen L. Study of the optimal control problem formulation for modulating air-to-water heat pumps connected to a residential floor heating system. Energy Build 2012;45(43–53). https://doi.org/10.1016/j.enbuild.2011.10.015 [Accessed on 12/01/2021]. Available from:.

[21] Sweetnam T, Fell M, Oikonomou E, Oreszczyn T. Domestic demand-side response with heat pumps: controls and tariffs. Build Res Inf 2019;47(4):344–61. https://doi.org/10.1080/09613218.2018.1442775 [Accessed on 12/01/2021]. Available from:.

[22] Franco A, Fantozzi F. Experimental analysis of a self consumption strategy for residential building: The integration of PV system and geothermal heat pump. Renew Energy 2016;86(1075–1085). https://doi.org/10.1016/j.renene.2015.09.030 [Accessed on 12/01/2021]. Available from:.

[23] Thygesen R, Karlsson B. Economic and energy analysis of three solar assisted heat pump systems in near zero energy buildings. Energy Build 2013;66(77–87). https://doi.org/10.1016/j.enbuild.2013.07.042 [Accessed on 12/01/2021]. Available from:.

[24] Prada A, Bee E, Grigiante M, Baggio P. On the optimal mix between lead-acid battery and thermal storage tank for PV and heat pump systems in high performance buildings. Energy Proc 2017;140(423–433). https://doi.org/10.1016/j.egypro.2017.11.154 [Accessed on 12/01/2021]. Available from:.

[25] Williams CJ, Binder JO, Kelm T. Demand side management through heat pumps, thermal storage and battery storage to increase local self-consumption and grid compatibility of PV systems. In: Innovative Smart Grid Technologies (ISGT Europe), 2012 3rd IEEE PES International Conference and Exhibition on. IEEE; 2012. p. 1–6. https://doi.org/10.1109/ISGTEurope.2012.6465874 [Accessed on 12/01/2021]. Available from:.

[26] Liu X, Zhang P, Pimm A, Feng D, Zheng M. Optimal design and operation of PV-battery systems considering the interdependency of heat pumps. J Energy Storage 2019;23:526–36. https://doi.org/10.1016/j.est.2019.04.026 [Accessed on 12/01/2021]. Available from:.

[27] Terlouw T, AlSkaif T, Bauer C, van Sark W. Optimal energy management in all-electric residential energy systems with heat and electricity storage. Appl Energy 2019;254:113580. [Accessed on 12/01/2021]. Available from: https://doi.org/10.1016/j.apenergy.2019.113580.

[28] Pimm AJ, Cockerill TT, Taylor PG. The potential for peak shaving on low voltage distribution networks using electricity storage. J Energy Storage 2018;16:231–42. https://doi.org/10.1016/j.est.2018.02.002 [Accessed on 12/01/2021]. Available from:.

[29] Tjaden T, Schnorr F, Weniger J, Bergner J, Quaschning V. Einsatz von PV-Systemen mit Wärmepumpen und Batteriespeichern zur Erhöhung des Autarkiegrades in Einfamilienhaushalten. In: 30. Symposium Photovoltaische Solarenergie; 2015. [Accessed on 12/01/2021]. Available from: https://doi.org/10.13140/RG.2.1.4033.9044.

[30] Schuetz P, Gwerder D, Gasser L, Fischer L, Wellig B, Worlitschek J. Thermal storage improves flexibility of residential heating systems for smart grids. In: Proceedings of the 12th IEA heat pump conference; 2017. p. 1–9.

[31] Dott R, Haller MY, Ruschenburg J, Ochs F, Bony J. The reference framework for system simulations of the IEA SHC Task 44/HPP Annex 38 Part B: buildings and space heat load. Int Energy Agency 2013;[Accessed on 12/01/2021]. Available from: http://www.taskx.iea-shc.org/data/sites/1/publications/T44A38_Rep_C1_B_ReferenceBuildingDescription_Final_Revised_130906.pdf.

[32] Arteconi A, Hewitt NJ, Polonara F. Domestic demand-side management (DSM): Role of heat pumps and thermal energy storage (TES) systems. Appl Therm Eng 2013;51(1–2):155–65.

[33] Vivian J, Prataviera E, Cunsolo F, Pau M. Demand Side Management of a pool of air source heat pumps for space heating and domestic hot water production in a residential district. Energy Convers Manag 2020;225:113457.

[34] Pena-Bello A, Barbour E, Gonzalez M, Patel M, Parra D. Optimized PV-coupled battery systems for combining applications: Impact of battery technology and geography. Renew Sustain Energy Rev 2019;112:978–90. https://doi.org/10.1016/j.rser.2019.06.003 [Accessed on 12/01/2021]. Available from:.

[35] Schuetz P, Scoccia R, Gwerder D, Waser R, Sturzenegger D, Elguezabal P, et al. Fast simulation platform for retrofitting measures in residential heating. In: Cold Climate HVAC Conference. Springer; 2018. p. 713–23. https://doi.org/10.1007/978-3-030-00662-4_60 [Accessed on 12/01/2021]. Available from:.

[36] Jordan U, Vajen K. Influence of the DHW load profile on the fractional energy savings: A case study of A solar combi-system with TRNSYS simulations. Solar Energy 2001;69:197–208.

[37] Villalva MG, Gazoli JR, Ruppert Filho E. Comprehensive approach to modeling and simulation of photovoltaic arrays. IEEE Trans Power Electron 2009;24(5):1198–208.

[38] Zhang Y, Lundblad A, Campana PE, Benavente F, Yan J. Battery sizing and rule-based operation of grid-connected photovoltaic-battery system: A case study in Sweden. Energy Convers Manag 2017;133:249–63.

[39] Sanyo Electric Co L. HIT photovoltaic module HIT-N2XXSE10 datasheet;. Available from: https://bit.ly/38OBh97.

[40] Duffie JA, Beckman WA. Solar engineering of thermal processes. John Wiley & Sons; 2013.

[41] Ineichen P. Solar radiation resource in Geneva: measurements, modeling, data quality control, format and accessibility. Archive ouverte Unige 2013;:from. https://www.unige.ch/sysener/fr/activites/meteo/acces-aux-donnees/.

[42] Bundesamt für Energie. Erneuerbare Energien Einspeisevergütung Berichte; 2018. [Accessed on 12/01/2021]. Available from: https://www.bfe.admin.ch/bfe/de/home/foerderung/erneuerbare-energien/einspeiseverguetung.html#kw-82976.

[43] Pfenninger S, Staffell I. Long-term patterns of European PV output using 30 years of validated hourly reanalysis and satellite data. Energy 2016;114:1251–65.

[44] Oualmakran Y, Espeche JM, Sisinni M, Messervey T, Lennard Z. Residential electricity tariffs in Europe: Current situation, evolution and impact on residential flexibility markets. Proceedings 2017;1(7). https://doi.org/10.3390/proceedings1071104 [Accessed on 12/01/2021]. Available from:.

[45] Azarova V, Engel D, Ferner C, Kollmann A, Reichl J. Exploring the impact of network tariffs on household electricity expenditures using load profiles and socio-economic characteristics. Nature Energy 2018;3(4):317. [Accessed on 12/01/2021]. Available from: https://doi.org/10.1038/s41560-018-0105-4.

[46] Bauer C, Hirschberg S, Bäuerle Y, Biollaz S, Calbry-Muzyka A, Cox B, et al. Potentials, costs and environmental assessment of electricity generation technologies. PSI, WSL, ETHZ, EPFL, Paul Scherrer Institut, Villigen, Switzerland. 2017;[Accessed on 12/01/2021]. Available from: https://www.psi.ch/sites/default/files/import/ta/HomeEN/Final-Report-BFE-Project.pdf.

[47] Hart WE, Laird C, Watson JP, Woodruff DL. Pyomo-optimization modeling in python. vol. 67. Springer; 2012. [Accessed on 12/01/2021]. Available from: https://doi.org/10.1007/978-3-319-58821-6.

[48] Hoval. Dimensionierungshilfe für Wärmepumpenanlagen 2017 Technische. Hoval; 2017.

[49] Gwerder D, Schuetz P. Machbarkeitsstudie zum Flexibilitätspotential von Wärmepumpen mit Speichern in Smart Grids. Bundesamt für Energie 2019.

[50] Berger M, Worlitschek J. A novel approach for estimating residential space heating demand. Energy 2018;159:294–301. https://www.sciencedirect.com/science/article/pii/S0360544218312039.

[51] Yao S, Gu W, Zhou S, Lu S, Wu C, Pan G. Hybrid timescale dispatch hierarchy for combined heat and power system considering the thermal inertia of heat sector. IEEE Access 2018;6:63033–44. https://doi.org/10.1109/ACCESS.2018.2876718.

[52] Swiss Society of Engineers and Architects. SIA 382/2 Klimatisierte Gebäude – Leistungs- und Energiebedarf. SIA; 2011.

[53] Fischer D, Lindberg KB, Madani H, Wittwer C. Impact of PV and variable prices on optimal system sizing for heat pumps and thermal storage. Energy Build 2016;128:723–33. https://doi.org/10.1016/j.enbuild.2016.07.008 [Accessed on 12/01/2021]. Available from:.

[54] Ardani K, O'Shaughnessy E, Fu R, McClurg C, Huneycutt J, Margolis R. Installed Cost Benchmarks and Deployment Barriers for Residential Solar Photovoltaics with Energy Storage: Q1 2016. Golden, CO: National Renewable Energy Laboratory (NREL). NREL/TP-7A40-67474; 2017. [Accessed on 12/01/2021]. Available from: https://www.nrel.gov/docs/fy17osti/67474.pdf.

[55] Schmidt T, Beuse M, Xiaojin Z, Steffen B, Schneider S, Pena-Bello A, et al. Additional emissions and cost from storing electricity in stationary battery systems. Environ Sci Technol 2019;53(7):3379–90. https://doi.org/10.1021/acs.est.8b05313 [Accessed on 12/01/2021]. Available from:.

[56] Toradmal A, Kemmler T, Thomas B. Boosting the share of onsite PV-electricity utilization by optimized scheduling of a heat pump using buildings thermal inertia. Appl Therm Eng 2018;137:248-258.

[57] Waser R, Berger M, Maranda S, Worlitschek J. Residential-scale demonstrator for seasonal latent thermal energy storage for heating and cooling application with optimized PV self-consumption. In: 2019 IEEE PES innovative smart grid technologies Europe (ISGT-Europe). IEEE; 2019. p. 1–5.

[58] Horowitz KA, Palmintier B, Mather B, Denholm P. Distribution system costs associated with the deployment of photovoltaic systems. Renew Sustain Energy Rev 2018;90:420–33.

[59] Blok K, Nieuwlaar E. Introduction to energy analysis. Routledge; 2016.

[60] Luthander R, Nilsson AM, Widén J, Åberg M. Graphical analysis of photovoltaic generation and load matching in buildings: A novel way of studying self-consumption and self-sufficiency. Appl Energy 2019;250:748–59. https://doi.org/10.1016/j.apenergy.2019.05.058 [Accessed on 12/01/2021]. Available from:.

[61] Royston J, Algorithm AS. 181: the W test for normality. Appl Stat 1982:176–80.

[62] Hollander M, Wolfe DA, Chicken E. Nonparametric statistical methods, vol. 751. John Wiley & Sons; 2013.

[63] Team, R Core and others. R. A language and environment for statistical computing. 2013.

[64] Narula K, Chambers J, Streicher KN, Patel MK. Strategies for decarbonising the Swiss heating system. Energy 2019;169:1119–1131. [Accessed on 12/01/2021]. Available from: http://www.sciencedirect.com/science/article/pii/S0360544218324484.

[65] Streicher KN, Padey P, Parra D, Bürer MC, Patel MK. Assessment of the current thermal performance level of the Swiss residential building stock: Statistical analysis of energy performance certificates. Energy Build 2018;178:360–78.

[66] Streicher KN, Mennel S, Chambers J, Parra D, Patel MK. Cost-effectiveness of large-scale deep energy retrofit packages for residential buildings under different economic assessment approaches. Energy Build 2020;215:109870.

[67] Hennig R, Jonker M, Tindemans S, De Vries L. Capacity subscription tariffs for electricity distribution networks: design choices and congestion management. In: 2020 17th international conference on the european energy market (EEM). IEEE; 2020. p. 1–6.

[68] AF-Mercados E. Study on tariff design for distribution systems. Technical Report.; 2015. Available from: https://ec.europa.eu/energy/sites/ener/files/documents/20150313%20Tariff%20report%20fina_revREF-E.PDF.

[69] Prettico G, Flammini M, Andreadou N, Vitiello S, Fulli G, Masera M. Distribution system operators observatory 2018. Publications Office of the European Union. 2019.
[70] Perez-Arriaga Ignacio J, Jenkins Jesse D, Batlle Carlos. A regulatory framework for an evolving electricity sector: Highlights of the MIT utility of the future study. Econ Energy Environ Policy 2017;6(1):71–92.
[71] Savelli Iacopo, Morstyn Thomas. Electricity prices and tariffs to keep everyone happy: A framework for fixed and nodal prices coexistence in distribution grids with optimal tariffs for investment cost recovery. Omega 2021;102450.
[72] Fridgen Gilbert, et al. One rate does not fit all: An empirical analysis of electricity tariffs for residential microgrids. Appl Energy 2018;210:800–14.
[73] Fu R, Feldman DJ, Margolis RM, Woodhouse MA, Ardani KB. US solar photovoltaic system cost benchmark: Q1 2017. Golden, CO: National Renewable Energy Laboratory (NREL). NREL/TP-6A20-68925; (2017). [Accessed on 12/01/2021]. Available from: https://www.nrel.gov/docs/fy17osti/68925.pdf.
[74] Burger B, Rüther R. Inverter sizing of grid-connected photovoltaic systems in the light of local solar resource distribution characteristics and temperature. Solar Energy 2006;80(1):32–45. https://doi.org/10.1016/j.solener.2005.08.012 [Accessed on 12/01/2021]. Available from:.
[75] Baumann T, Baumgartner F. Home Batteriespeicher, studie für solarspar. ZHAW/IEFE; 2017. [Accessed on 12/01/2021]. Available from: https://www.solarspar.ch/app/download/12621170687/20170106_Home_Batteriespeicher_solarspar.pdf?t=1569512414.